Metal–Organic Frameworks

DOI: 10.1002/ange.201101924

# Sequential Functionalization of Porous Coordination Polymer Crystals**

*Kenji Hirai, Shuhei Furukawa,* Mio Kondo, Hiromitsu Uehara, Osami Sakata, and Susumu Kitagawa**

Chemists fabricate multifunctional materials by integrating two or more distinct chemical functionalities into a single platform. This structural complexity allows the design of materials that possess contradictory properties. These materials have integrated properties that conventional single-phase materials can never achieve.[1] The key to this integration is arranging the chemical functionalities at the desired positions within the material. Organic polymer chemistry has shown that the spatial arrangement of functionalities determines the resulting properties, with a homogeneous distribution resulting in a mixed and a heterogeneous distribution leading to the formation of a separated phase. Whereas random copolymers with several chemical functionalities display functions that are different from their original ones, block copolymers that partition the chemically distinct phases lead to the coexistence of individual properties.[2] Herein, we introduce heterogeneity into hybridization systems of coordination polymers to fabricate multifunctional porous materials that synergistically exhibit two contradictory porous properties.

Porous coordination polymers (PCPs), or metal–organic frameworks (MOFs), form three-dimensional molecular skeletons consisting of organic spokes and inorganic nodes.[3] PCPs are an intriguing class of porous crystalline materials in which the properties can be modulated simply by altering the chemical functionalities on the organic spokes.[4] The porous properties can be controlled by introducing appropriate substituents. Pore size is affected by ligand bulkiness,[5] specific chemical affinity is affected by hydrogen bonding,[6] and reactivity is affected by the isolation or exposure of the reactive site.[7] The porous functions of PCPs can be broadly divided into two classes based on different length scales. Spatial function, such as storage or size selectivity, originate from the space surrounded by the framework scaffold, where the arrangement of chemical functionalities dominates the function. In contrast, local functions, such as reactivity or catalytic activity, arise from the chemical structure of components, such as open metal sites[8] or reactive organic sites.[9]

Although local functions can be integrated into a mixed homogeneous phase of PCPs using several organic linkers, homogeneous integration alters spatial functions owing to the random arrangement of organic linkers.[10,11] One way to overcome this issue is to prepare heterogeneous structures containing bimodal pore networks. The simple but sequentially arranged hybridization of single PCP crystals affords control over the sequence of individual spatial functions. Such heterogeneous structured PCPs enable multifunctionality even when two contradictory properties are combined (Figure 1), such as small and large pore sizes providing a simultaneous size selectivity and storage. Large cavities are essential to achieve a high storage capacity but accept any guest molecule, thus sacrificing size selectivity. To overcome this limitation, a platform could be designed containing both crystal A (small aperture) and B (large cavity) for separation and storage, respectively.

One of the most promising applications of PCPs is gas and liquid separation using column packing materials[12] or separation membranes.[13] Although these separation systems exhibit excellent performance with dynamically flowing mixtures, there is also a need to separate one substrate from a mixture under static conditions, such as for biological systems or in a fuel tank. The extraction of byproducts, impurities, or toxic substances in these sorts of system requires a single material that can be used for the sequential separation and accumulation of the extracted product.

Herein, the fabrication of a single-crystal extractor based on PCPs with core–shell heterostructures is presented in which the storage container is the core crystal and the size separation filter is the shell crystal. The design of isoreticular frameworks with organic ligands of different sizes allows the

[*] K. Hirai, Prof. S. Kitagawa
Department of Synthetic Chemistry & Biological Chemistry
Graduate School of Engineering, Kyoto University
Katsura, Nishikyo-ku, Kyoto 615-8510 (Japan)
Fax: (+81) 75-383-2732
E-mail: kitagawa@sbchem.kyoto-u.ac.jp

Dr. S. Furukawa, Dr. H. Uehara, Prof. S. Kitagawa
ERATO Kitagawa Integrated Pores Project
Japan Science and Technology Agency (JST)
Kyoto Research Park Bldg no. 3, Shimogyo-ku
Kyoto 600-8815, (Japan)
Fax: (+81) 75-325-3572
E-mail: shuhei.furukawa@kip.jst.go.jp

Dr. S. Furukawa, Dr. M. Kondo, Prof. S. Kitagawa
Institute for Integrated Cell-Material Sciences (iCeMS)
Kyoto University, Yoshida, Sakyo-ku, Kyoto 606-8501 (Japan)

Dr. O. Sakata
Research & Utilization Division
Japan Synchrotron Research Institute/Spring-8 and CREST, JST
Kouto, Sayo, Hyogo 679-5198 (Japan)

[**] K.H. is grateful to JSPS Research Fellowships for Young Scientists. The synchrotron X-ray experiments were performed at BL13XU in the SPring-8 with the approval of the JASRI (Proposal No. 2010A1597). We acknowledge Prof. I. Hamachi, Dr. A. Ojida, and Dr. M. Ikeda (Kyoto Univ.) for assistance with confocal laser scanning microscopy measurements.

Supporting information for this article is available on the WWW under http://dx.doi.org/10.1002/anie.201101924.

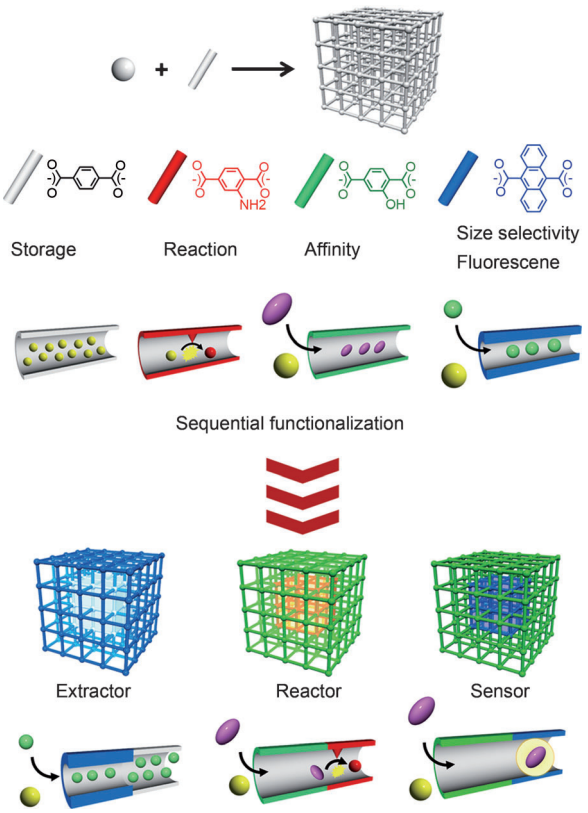


***Figure 1.*** Porous coordination polymer crystal hybridization for sequential functionalization systems.

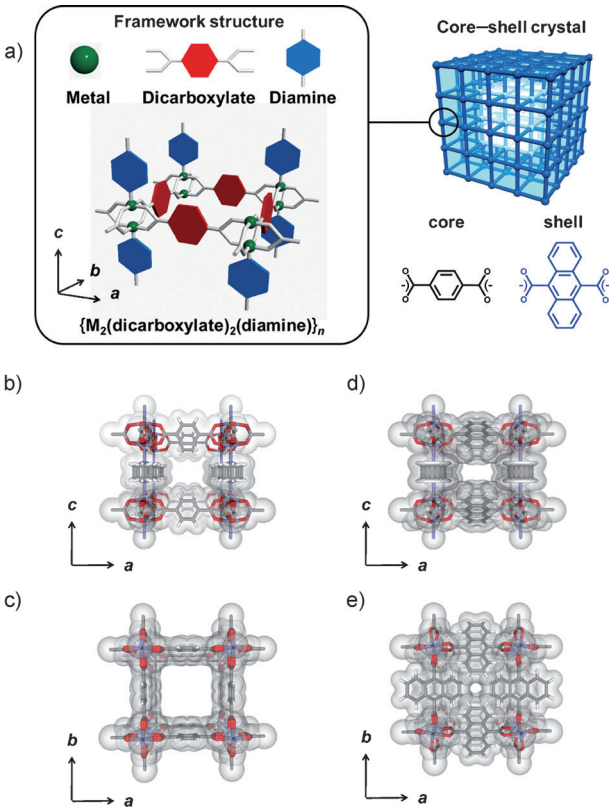


***Figure 2.*** a) A series of frameworks, $\{M_2(dicarboxylate)_2(diamine)\}_n$. The crystal structure of **1** viewed along b) the *b* axis and c) the *c* axis. The structure of **2** viewed along d) the *b* axis and e) the *c* axis.

connection of pores at the interfaces between the two PCP crystals by epitaxial growth. We demonstrate the crystal extractor using the extraction of cetane (*n*-hexadecane) from its branched isomer, isocetane (2,2,4,4,6,8,8-heptamethylnonane), both of which are important molecules in diesel fuels.[14] Even at a low concentration of cetane (<1%), the sequentially hybridized PCP crystals only extract cetane from the mixture, which allows it to accumulate in the large pores of the core container.

A series of three-dimensional PCPs, $\{Zn_2(dicarboxylate)_2(dabco)\}_n$,[15] gives a single micrometer-scale crystal with a well-defined cuboid morphology in which the dicaroboxylate layer ligands link to the zinc paddlewheel clusters to form two-dimensional square lattices connected by dabco pillar ligands at the lattice points (dabco = 1,4-diazabicyclo-[2.2.2]octane). The single-crystalline nature is essential for achieving sequential growth of the second crystal on the crystal surface. As the significant differences in pore sizes and surface areas between the core and shell crystals leads to the fabrication of the crystal extractor, we selected $\{Zn_2(bdc)_2(dabco)\}_n$[15b] (**1**) as the core framework (bdc = 1,4-benzene dicarboxylate; pore sizes $7.5\times7.5$ Å$^2$ along the *c* axis, $5.3\times3.2$ Å$^2$ along the *a* and *b* axes; micropore volume 0.75 cm$^3$ g$^{-1}$) and $\{Zn_2(adc)_2(dabco)\}_n$[15d] (**2**) as the shell framework (adc = 9,10-anthracene dicarboxylate; pore sizes $1.7\times1.7$ Å$^2$ along the *c* axis, $4.5\times2.7$ Å$^2$ along the *a* and *b* axes; micropore volume 0.31 cm$^3$ g$^{-1}$). This system is shown in Figure 2 and in the Supporting Information, Figure S1.

Two frameworks were successfully hybridized into one crystal by a simple solvothermal synthesis.[16] Pieces of single crystals of **1** were placed into a solution of $Zn(NO_3)_2\cdot6H_2O$, 9,10-anthracene dicarboxylic acid, and dabco in *N*,*N*-dimethylformamide (DMF), and the solution was heated to 393 K for three days. The core–shell crystals (**1**/**2**) were harvested after cooling to room temperature.

Because both crystalline phases are colorless, it is inherently difficult to distinguish between the two phases using an optical microscope; therefore, we used a confocal laser scanning microscope (CLSM) with anthracene fluorescent emission as a probe to determine the three-dimensional configuration of the core–shell crystals. Horizontally sliced CLSM images at two different focal points are shown in the Supporting Information, Figure S2. Whereas the image slice from the focal point at the bottom of the crystal showed fluorescence across the whole surface, the image slice from the focal point at the middle of the crystal gave an image with fluorescence on only four sides of the crystal (Figure 3a). The CLSM images at different focal points indicated that the shell crystals of **2** covered all the surfaces of the core crystal **1**.

We also used microscopic laser Raman spectroscopy (MLRS) to examine core–shell crystals mechanically sliced at the middle of the crystal. As shown in Figure 3c–f, mapping according to characteristic Raman signals corresponding to the core and shell framework (colored red and green, respectively, in Figure 3b) supported the formation of a

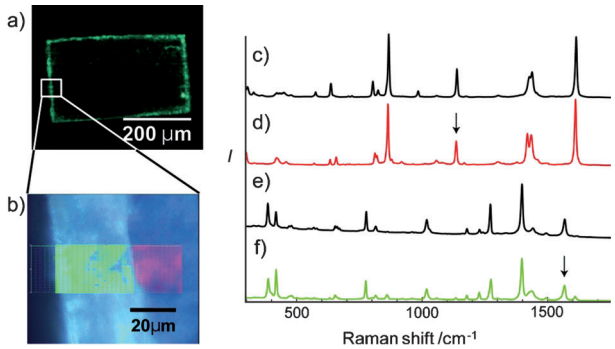


***Figure 3.*** a) A horizontally sliced CLSM image at the focal point at the middle of the crystal. b) The Raman mapping for the mechanically sliced core–shell crystal at the middle of the crystal. Raman spectra obtained from c) a single crystal of **1**, d) the core part of **1/2**, e) a single crystal of **2**, and f) the shell part of **1/2**. Arrows indicate the characteristic Raman signal corresponding to **1** and **2** that were used for the mapping in (b).

core–shell crystal with microscopically abrupt interfaces. The Raman mapping measurement indicated that the shell crystals was several tenths of a micrometer in thickness. The molar ratio of the core framework to the shell framework was determined to be 8:2 by $^1$H NMR spectroscopy of core–shell crystals that had been decomposed with hydrochloric acid (Supporting Information, Figure S3). Furthermore, synchrotron X-ray diffraction measurements for film structural analysis revealed that the hybridization of two frameworks into one crystal with pore connections at the crystal interfaces had been achieved (Supporting Information, Figures S4–S6).

We tested the accessibility of the guest petroleum molecules to the core crystal though the shell crystal. The guest-free core–shell crystals of **1/2** were separately immersed into either cetane or isocetane for a week. After filtration and drying, the MLRS technique was used to detect the characteristic signals of petroleum molecules inside the core crystal in the range 2600–3100 cm$^{-1}$ [17] (Figure 4). The Raman signal of cetane was observed when the excitation laser was focused at the core crystal, which suggested the successful travel of cetane through the pores of the shell framework and the crystal interfaces (Figure 4 e,g). In contrast, no Raman signal indicative of isocetane was detected in either the core or shell crystals (Figure 4 f,h). This result indicates that the shell crystal restricts the adsorption of isocetane. When a single crystal of **2** was immersed into isocetane, no Raman signal was observed either (Figure 4 d). Therefore, the bulkier branched isocetane was blocked by the steric effect of the small aperture of **2**. Note that this blocking indicated that there was no cracks or defects in the shell crystal that isocetane can pass through.

The preference for adsorbing cetane over isocetane was demonstrated by immersing single crystals of **1** and **2** and a core–shell crystal of **1/2** into a mixture of cetane/isocetane (1:1). After filtration and drying, these crystals were decomposed by hydrochloric acid and the adsorption ratio was determined by gas chromatography-mass spectrometry (GC-MS; Supporting Information, Figure S7). Branched isocetane (with a retention time of 2.72 min) was eluted from the GC column before its linear isomer cetane (with a retention time of 3.98 min). Whereas the large pores of **1** barely discriminated between these isomers, the small pores of **2** accumulated only the linear cetane molecules. The core–shell crystal also selectively adsorbed cetane owing to the small aperture of the shell crystal. When the cetane/isocetane ratio was decreased to 1:10 and 1:100 (Supporting Information, Figure S8, and Figure 5 a, respectively), the adsorption of isocetane in **1** increased. In contrast, the crystal of **2** and the core–shell crystal **1/2** maintained their selective adsorption of cetane.

The storage capacity of cetane in the core–shell crystal of **1/2** was elucidated by thermogravimetric (TG) analysis. Because the weight loss of both the guest petroleum molecules and dabco[18] from the framework occurred from 250–330 °C, the weight loss from the guest molecules was calculated by subtracting the contribution of dabco from the total weight loss (Supporting Information, Figure S9 and 10 and Table S1). For the 1:100 mixture of cetane/isocetane, the amount of cetane adsorbed in the core–shell crystal was estimated to be 26.9 wt %, which was twice that in the shell crystal of **2** (10.0 wt %; Figure 5 b). This significant improvement in the cetane storage capacity arose from the large pore

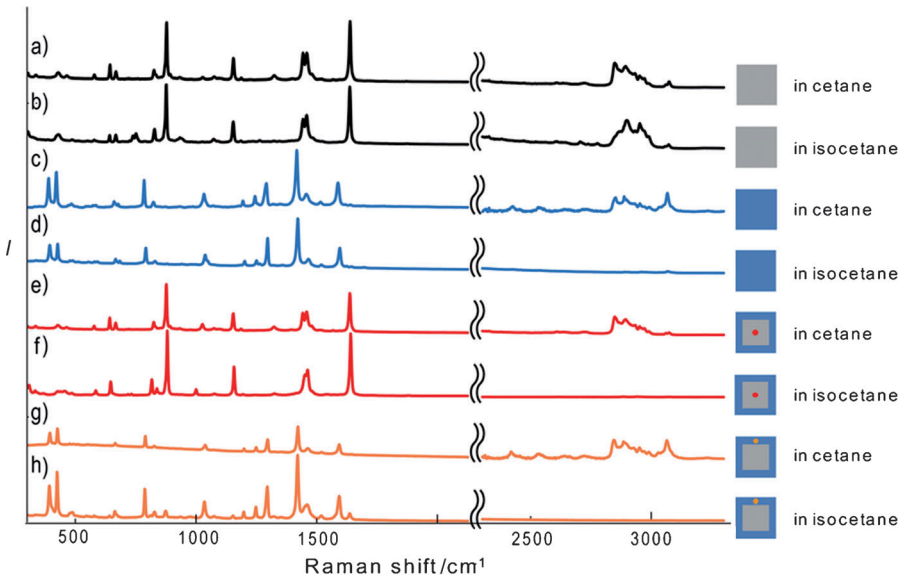


***Figure 4.*** Raman spectra obtained from single crystals of **1** immersed in a) cetane and b) isocetane, single crystals of **2** immersed in c) cetane and d) isocetane, the core portion of **1/2** immersed in e) cetane and f) isocetane, and from the shell portion of **1/2** immersed in g) cetane and h) isocetane. The red and orange points in the core–shell crystal of **1/2** indicates the point at which the Raman laser is focused.

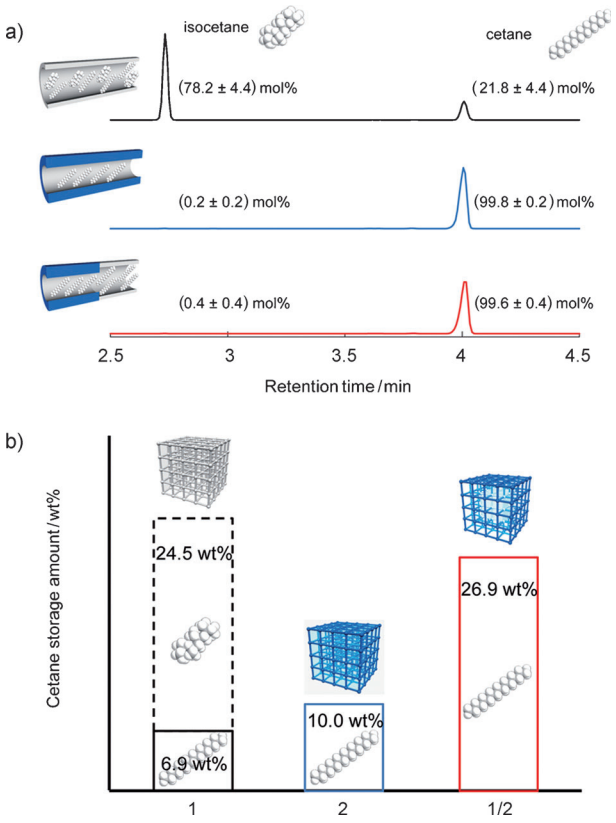


***Figure 5.*** a) The selective adsorption of cetane over isocetane from mixtures with a cetane/isocetane ratio of 1:100 as determined by GC-MS. The core–shell crystal only accumulated cetane (bottom) owing to the small pores of the shell crystal of **2** (middle); in contrast, isocetane was preferentially adsorbed by crystals of **1** (top). b) The amount of cetane stored in **1**, **2**, and **1/2** when using a 1:100 mixture of cetane/isocetane.

volume of the core framework of **1**. In contrast, the single crystal of **1** alone showed no selective adsorption, and both cetane (6.9 wt%) and isocetane (24.5 wt%) accumulated in its pores. Thus, covering the core crystal with the thin shell crystal is the key to the combination of selectivity for cetane and high storage capacity.

In conclusion, we have succeeded in sequential functionalization of PCP crystals by fabricating core–shell type heterostructures that exhibited size selectivity owing to the small aperture of the shell framework and high storage capacity owing to the large pore volume of the core framework. This successful integration of two contradictory spatial functions into one crystal was enabled by the heterogeneous arrangement of chemical functionalities on one basic framework skeleton. This first example of a multifunctional PCP crystal will enable further integration of other porous properties.

## *Experimental Section*

Anhydrous DMF, $Zn(NO_3)_2{\cdot}6H_2O$, dabco, *n*-hexadecane, 2,4,4,6,8,8-heptametylnonane, *n*-hexane, and aqueous hydrochloric acid were purchased from Wako Pure Chemical Industries. 9,10-anthracenedicarboxylic acid ($H_2adc$) was prepared according to a previously published procedure.[19]

Compound **1** was prepared according to previously published procedures.[15b] The reaction solution for **2** was prepared from $Zn(NO_3)_2{\cdot}6H_2O$ (0.100 mg, 0.336 mmol), adc (0.089 mg, 0.336 mmol), and dabco (0.019 mg, 0.167 mmol) in DMF (4 mL). Dozens of single crystals of **1** were added to a 4 mL reaction solution. The reaction mixture was then heated to 393 K and maintained at that temperature for 3 days. After cooling, the coreless hybridized crystals of **1/2** were harvested.

Confocal laser scanning microscopy: The core–shell crystals (**1/2**) were immersed into DMF solvent and placed on a glass substrate. The fluorescence images at different depths were obtained by a FV1000 microscope (Olympus) with a semiconductor laser at 370 nm, and fluorescent emission was collected in the 400–430 nm range.

The Raman spectra were measured by a LabRAM HR-800 spectrometer (Horiba Jobin Yvon Ltd.) with a semiconductor laser at 785 nm. The single crystal samples of **1**, **2**, or **1/2** were placed on the glass substrate. Gas chromatography mass spectrometry (GC-MS) was performed using a SHIMADZU QP2010 with a DB-5MS capillary column (length 30 m, film thickness 0.25 mm, Agilent Technologies). The following conditions were employed: electron energy 70 eV, scan range from *m/z* 50 to 276 in 0.5 s, ion source temperature 200 °C, transfer line temperature 200 °C, injector temperature 300 °C, column temperature 200 °C for 5 min, and He carrier gas flow rate 0.51 mL $min^{-1}$. The crystals, which were immersed in the cetane/isocetane mixture, were decomposed by aqueous hydrochloric acid and all alkane molecules were extracted by *n*-hexane solvent. After the extraction, the adsorption ratio of cetane/isocetane was analyzed by GC-MS. Thermogravimetric (TG) analyses were performed using a Rigaku Thermo plus TG 8120 apparatus in the temperature range between 303 K and 773 K in a $N_2$ atmosphere and at a heating rate of 10 K $min^{-1}$.

Received: March 18, 2011
Published online: July 14, 2011

**Keywords:** crystal growth · metal–organic frameworks · porous coordination polymers · separation · surface modification

[1] E. Katz, I. Willner, *Angew. Chem.* **2004**, *116*, 6166 – 6235; *Angew. Chem. Int. Ed.* **2004**, *43*, 6042 – 6108.
[2] D. E. Discher, A. Eisenberg, *Science* **2002**, *297*, 967 – 973.
[3] a) S. R. Batten, R. Robson, *Angew. Chem.* **1998**, *110*, 1558 – 1595; *Angew. Chem. Int. Ed.* **1998**, *37*, 1460 – 1494; b) O. M. Yaghi, M. O'Keeffe, N. W. Ockwig, H. K. Chae, M. Eddaoudi, J. Kim, *Nature* **2003**, *423*, 705 – 714; c) S. Kitagawa, R. Kitaura, S. Noro, *Angew. Chem.* **2004**, *116*, 2388 – 2430; *Angew. Chem. Int. Ed.* **2004**, *43*, 2334 – 2375; d) G. Férey, C. Serre, *Chem. Soc. Rev.* **2009**, *38*, 1380 – 1399.
[4] a) J. S. Seo, D. Whang, H. Lee, S. I. Jun, J. Oh, Y. J. Jeon, K. Kim, *Nature* **2000**, *404*, 982 – 986; b) X. Zhao, B. Xiao, A. J. Fletcher, K. M. Thomas, D. Bradshaw, M. J. Rosseinsky, *Science* **2004**, *306*, 1012 – 1015; c) S. Bureekaew, S. Horike, M. Higuchi, M. Mizuno, T. Kawamura, D. Tanaka, N. Yanai, S. Kitagawa, *Nat. Mater.* **2009**, *8*, 831 – 836; J. A. Hurd, R. Vaidhyanathan, V. Thangadurai, C. I. Ratcliffe, I. L. Moudrakovski, G. K. H. Shimizu, *Nat. Chem.* **2009**, *1*, 705 – 710; d) O. Shekhah, H. Wang, M. Paradinas, C. Ocal, B. Schüpbach, A. Terfort, D. Zacher, R. A. Fischer, C. Wöll, *Nat. Mater.* **2009**, *8*, 481 – 484; e) Y. Inokuma, T. Arai, M. Fujita, *Nat. Chem.* **2010**, *2*, 780 – 783; f) D. Maspoch, D. Ruiz-Molina, K. Wurst, N. Domingo, M. Cavallini, F. Biscarini, J. Tejada, C. Rovira, J. Veciana, *Nat. Mater.* **2003**, *2*, 190 – 195; g) B. Xiao, P. J. Byrne, P. S. Wheatley, D. S. Wragg, X. Zhao, A. J.

Fletcher, K. M. Thomas, L. Peters, J. S. O. Evans, J. E. Warren, W. Zhou, R. E. Morris, *Nat. Chem.* **2009**, *1*, 289 – 294; h) J. R. Li, H. C. Zhou, *Nat. Chem.* **2010**, *2*, 893 – 898; i) O. K. Farha, O. Yazaydın, I. Eryazici, C. Malliakas, B. Hauser, M. G. Kanatzidis, S. T. Nguyen, R. Q. Snurr, J. T. Hupp, *Nat. Chem.* **2010**, *2*, 944 – 948; j) S. Yang, X. Lin, A. J. Blake, G. S. Walker, P. Hubberstey, N. R. Champness, M. Schröder, *Nat. Chem.* **2009**, *1*, 487 – 493; k) Z. Wang, S. M. Cohen, *Chem. Soc. Rev.* **2009**, *38*, 1315 – 1329; l) T. Devic, P. Horcajada, C. Serre, F. Salles, G. Maurin, B. Moulin, D. Heurtaux, G. Clet, A. Vimont, J.-M. Grenèche, B. Le Ouay, F. Moreau, E. Magnier, Y. Filinchuk, J. Marrot, J.-C. Lavalley, M. Daturi, G. Férey, *J. Am. Chem. Soc.* **2010**, *132*, 1127 – 1136.

[5] R. Banerjee, H. Furukawa, D. Britt, C. Knobler, M. O'Keeffe, O. M. Yaghi, *J. Am. Chem. Soc.* **2009**, *131*, 3875 – 3877.

[6] R. Matsuda, R. Kitaura, S. Kitagawa, Y. Kubota, R. V. Belosludov, T. C. Kobayashi, H. Sakamoto, T. Chiba, M. Takata, Y. Kawazoe, Y. Mita, *Nature* **2005**, *436*, 238 – 241.

[7] H. Sato, R. Matsuda, K. Sugimoto, M. Takata, S. Kitagawa, *Nat. Mater.* **2010**, *9*, 661 – 666.

[8] M. Dincã, A. Dailly, Y. Liu, C. M. Brown, D. A. Neumann, J. R. Long, *J. Am. Chem. Soc.* **2006**, *128*, 16876 – 16883.

[9] S. Hasegawa, S. Horike, R. Matsuda, S. Furukawa, K. Mochizuki, Y. Kinoshita, S. Kitagawa, *J. Am. Chem. Soc.* **2007**, *129*, 2607 – 2614.

[10] H. Deng, C. J. Doonan, H. Furukawa, R. B. Ferreira, J. Towne, C. B. Knobler, B. Wang, O. M. Yaghi, *Science* **2010**, *327*, 846 – 850.

[11] T. Fukushima, S. Horike, Y. Inubushi, K. Nakagawa, Y. Kubota, M. Takata, S. Kitagawa, *Angew. Chem.* **2010**, *122*, 4930 – 4934; *Angew. Chem. Int. Ed.* **2010**, *49*, 4820 – 4824.

[12] a) B. Chen, C. Liang, J. Yang, D. S. Contreras, Y. L. Clancy, E. B. Lobkovsky, O. M. Yaghi, S. Dai, *Angew. Chem.* **2006**, *118*, 1418 – 1421; *Angew. Chem. Int. Ed.* **2006**, *45*, 1390 – 1393; b) B. Wang, A. P. Côté, H. Furukawa, M. O'Keeffe, O. M. Yaghi, *Nature* **2008**, *453*, 207 – 212; c) L. Alaerts, C. E. A. Kirschhock, M. Maes, M. A. van der Veen, V. Finsy, A. Depla, J. A. Martens, G. V. Baron, P. A. Jacobs, J. F. M. Denayer, D. E. De Vos, *Angew. Chem.* **2007**, *119*, 4371 – 4375; *Angew. Chem. Int. Ed.* **2007**, *46*, 4293 – 4297.

[13] H. Bux, F. Liang, Y. Li, J. Cravillon, M. Wiebcke, J. Caro, *J. Am. Chem. Soc.* **2009**, *131*, 16000 – 16001.

[14] a) G. Knothe, A. C. Matheaus, T. W. Ryan III, *Fuel* **2003**, *82*, 971 – 975; b) L. Xing-cai, Y. Jian-guang, Z. Wu-gao, H. Zhen, *Fuel* **2004**, *83*, 2013 – 2020.

[15] a) K. Seki, W. Mori, *J. Phys. Chem. B* **2002**, *106*, 1380 – 1385; b) D. N. Dybtsev, H. Chun, K. Kim, *Angew. Chem.* **2004**, *116*, 5143 – 5146; *Angew. Chem. Int. Ed.* **2004**, *43*, 5033 – 5036; c) B. Q. Ma, K. L. Mulfort, J. T. Hupp, *Inorg. Chem.* **2005**, *44*, 4912 – 4914; d) D. Tanaka, S. Horike, S. Kitagawa, M. Ohba, M. Hasegawa, Y. Ozawa, K. Toriumi, *Chem. Commun.* **2007**, 3142 – 3144.

[16] S. Furukawa, K. Hirai, K. Nakagawa, Y. Takashima, R. Matsuda, T. Tsuruoka, M. Kondo, R. Haruki, D. Tanaka, H. Sakamoto, S. Shimomura, O. Sakata, S. Kitagawa, *Angew. Chem.* **2009**, *121*, 1798 – 1802; *Angew. Chem. Int. Ed.* **2009**, *48*, 1766 – 1770.

[17] R. G. Snyder, H. L. Strauss, C. A. Elllger, *J. Phys. Chem.* **1982**, *86*, 5145 – 5150.

[18] Z. Chen, S. Xiang, D. Zhao, B. Chen, *Cryst. Growth Des.* **2009**, *9*, 5293 – 5296.

[19] S. Jones, C. J. Atherton, R. J. M. Elsegood, W. Clegg, *Acta Crystallogr. Sect. C* **2000**, *56*, 881 – 883.

  